CLASSIFICATION OF RAINFALL RADAR IMAGES USING THE SCATTERING TRANSFORM

Gerard Busquets Garcia, Mathieu Lagrange

IRCCYN CNRS, Ecole Centrale de Nantes
1, rue de la Noé, 44000 Nantes
(mathieu.lagrange@cnrs.fr)

Isabelle Emmanuel, Hervé Andrieu

PRES LUNAM, IFSTTAR,
Laboratoire Eau et Environnement,
and IRSTV FR CNRS 2488, Bouguenais

ABSTRACT

The main objective of this paper is to classify rainfall radar images by using the scattering transform, which gives us a translation invariant representation of the images and preserves high-frequency information useful to encode important morphological aspects of the meteorological phenomena under study. To demonstrate the usefulness of the approach, a classification framework is considered, where the images are to be classified into 4 morphological classes: light rain, shower, unorganised storm and organised storm. Experiments show that the benefits of the scattering are threefold: 1) it provides complementary information with respect to more traditional features computed over the distribution of the rainfall intensities, 2) it provides strong invariance to deformations, 3) second order coefficients of the scattering transform nicely encodes spatial distribution of rain intensity.

Index Terms— Classification, scattering, image radar processing

1. INTRODUCTION

Detection of the type of rainfall is interesting for urban hydrology. Depending on the type of rainfall, the water will spread very differently into the urban surfaces thus leading to different management options. From light rain to storms, the morphology of the meteorological phenomena can be very different. This variability occurs also within each class of rainfall.

Radar rainfall images are therefore a very challenging case-study for feature design. Even though spatial information is important to model as it conveys the structure of the meteorological phenomenon under interest, it has to be taken into account that invariance to translation, rotation and small deformations are also desirable. Indeed, each meteorological phenomenon will go through the radar area in different locations and angles, and its shape will vary while preserving global properties that can easily be recognized by a trained human. Those properties are non trivially expressed by the actual images. Some studies modeled rainfall fields as fractals [1, 2] or with spatial variograms [3], with, to the best of our knowledge, no application to feature design for rain type classification.

We propose in this paper to tackle this issue by considering the scattering framework proposed by Mallat [4]. This framework features most of the invariance constraints expressed above and has shown high performance in texture classification [5], thanks to its ability to model structured shapes by incorporating high order moments which can discriminate non-Gaussian properties.

The remaining of the paper is organized as follows. Section 2 presents some background information on the case study with the main characteristics of the 4 types of rainfalls as well as previously proposed features that consider the distribution of the rain intensity. Section 3 and 4 explain how the scattering transform works and how this new approach can help us to classify those images. Finally, section 5 shows the performance of the scattering transform and its complementarity with intensity distribution statistics.

2. BACKGROUND

The data considered in this study have been analyzed in [3] and highlighted at the mesoscale (ranging horizontally from around 5 kilometers to several hundred kilometers), three categories of meteorological situations: warm sectors, front and tail end of low pressure systems. Those meteorological situations give four different types of rainfall fields:

- Light rain (linked to warm sectors).
- Showers (linked to tail end of low pressure systems).
- Storms less organized (linked to fronts).
- Storms organized in rain bands (linked to fronts).

2.1. Typology of rainfall

In order to discriminate between those phenomena, some morphological aspects can be underlined:

Light rain: has few number of no-rain areas. However, in these rainy areas, the intensity is generally low compared

978-0-9928626-3-3/15/$31.00 ©2015 IEEE

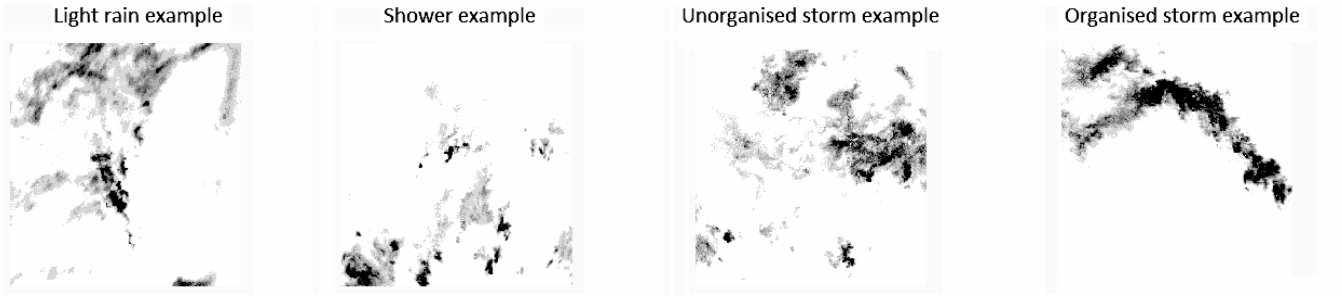

Fig. 1. The 4 types of rainfall.

with the other rain types.

Shower: can be considered as the opposite case of the light rain. The rain takes up little space in the area, but it has generally higher variance, which also turns into higher intensity.

Unorganised storms: storms that share some characteristics with showers. They are characterized by spread areas with both high and low intensities, that are somewhat disorganized.

Organised storms: storms that are characterized by large bands, which have both high and low intensities with higher rain intensity in the middle of the band.

The image database is formed by rain periods. Each rain period contains a group of images which show the rain intensity every 5 minutes in the incidence zone of the radar [6]. The images display an area of 40X50 km and every pixel gives the data of the rain intensity for 250X250m. 0 indicates a lack of rain. The higher the intensity, the higher the number is. In total, there are 34 rain periods for a total of 1239 images [3, 7].

The images have been received from the Treillieres radar, a C-band radar from the ARAMIS network located 10 km north from Nantes. A meteorological analysis has been already performed with the Centre Départemental de Loire-Atlantique de Météo France.

2.2. Distribution of rainfall intensity

As a baseline approach, one may consider some statistics which encode some aspects of the Rainfall Intensity Distribution (RID) as proposed in [3]:

- percentage of very small values (thresholded according to the radar sensitivity)

And with the remaining positive-valued intensities:

- mean of the intensity's values
- standard deviation
- median value

Table 1 shows the average values of those statistics for the four types of rainfall. Using those statistics which only encode the distribution of the intensity without any spatial information, we can see that the light rain has the lowest mean and zeros percentage. It means that light rain takes up more area than other kind of rain, but with lower intensity. This will make the light rain the easiest class to discriminate. On contrary, showers and unorganized storms will be the most difficult classes to discriminate, as they have very similar statistics.

In order to discriminate these two kind of rains, we have to consider other features that take into account the spatial configuration of the meteorological phenomenon. Section 3 will explain the scattering transform, which will allow us to achieve a better classification by providing this needed extra information.

3. SCATTERING TRANSFORM

To improve classification outcomes we represent the image using the scattering transform. An expected scattering representation of stationary processes is introduced for texture discrimination. As opposed to the Fourier power spectrum, it gives information on higher order moments, and can thus discriminate non-Gaussian textures having the same power spectrum. A scattering transform computes a translation invariant representation by cascading wavelet transforms and modulus pooling operators, which average the amplitude of iterated wavelet coefficients. It is also Lipschitz continuous to deformations, while preserving the signal energy [4].

A scattering transform builds non-linear invariants from wavelet coefficient, with modulus and averaging pooling functions.

Being G a group of rotations r of angles $2k\pi/K$ for $0 \leq k < K$ two-dimensional directional wavelets are obtained by rotating a single band-pass filter ψ by $r \in G$ and dilating it by 2^j for $j \in Z$ (where j is the scale in the filter). More translation invariant coefficients can be obtained by further iterating on the wavelet transforms and modulus operators. Let $U[\lambda]x = |x \star \psi_\lambda|$. Any sequence $p = (\lambda_1, \lambda_2, , \lambda_m)$ defines a path along which is computed an ordered product of

	% Zeros	Mean	Std Dev	Median
Rain	28,7 (5,0)	1,2 (0,5)	1,1 (0,4)	0,9 (0,4)
Shower	79,7 (1,3)	3,4 (6,0)	7,6 (35,3)	0,9 (0,2)
O. storm	56,1 (0,4)	7,3 (16,9)	14,2 (77,2)	2,5 (0,9)
U. storm	67,8 (2,0)	3,0 (4,2)	6,3 (22,7)	1,1 (0,4)

Table 1. Mean and variance of the RID statistics computed over the different rainfall types.

non-linear and non-commuting operators [5].

$$U[p]x = U[\lambda_m]...U[\lambda_2]U[\lambda_1]x = |x \star \psi_1||x \star \psi_2|...|x \star \psi_m|$$

A Scattering transform along the path p is defined as an integral, normalized by the response of a Dirac:

$$S_x[p] = \mu_p^{-1} \int U[p]x(u)du \;\; with \;\; \mu_p = \int U[p]\delta(u)du$$

Each Scattering coefficient is invariant to translation of x. Considering classification tasks, it is often better to compute localized descriptors, which are invariant to translations, smaller than a predefined scale 2^J, while keeping the spatial variability at scales larger than 2^j. This is obtained by localizing the scattering integral with a scaled spatial window[5]:

$$\phi_{2^J}(u) = 2^{-2J}\phi(2^{-J}u)$$

It defines a windowed scattering transform in the neighborhood of u:

$$S[p]x(u) = U[p]x \star \phi_{2^J}(u) = \int U[p]x(v)\phi_{2^J}(u-v)dv$$

And hence:

$$S[p]x(u) = |x \star \psi_1||x \star \psi_2||x \star \psi_m|\phi_{2^J}(u)$$

$S[p]x(u)$ is a function of the window position u, which can be sub-sampled at intervals proportionate to the window size2^J.

If $p = (\lambda_1, \lambda_m)$ is a path of length m then $S[p]x(u)$ is called a windowed scattering coefficient of order m. It is computed at the layer m of the specified convolution network. For large scale invariants, several layers are necessary to avoid losing crucial information. For appropriate wavelets, first order coefficients $S[_1]x$ are equivalent to scale-invariant feature transform (SIFT) coefficients as it computes the local sum of image gradient amplitudes among image gradients having nearly the same direction in a histogram having 8 different direction bins [8]. A Scattering transform computes higher-order coefficients by further iterating on wavelet transforms and modulus operators. Wavelet coefficients are computed up to a maximum scale 2^J and the lower frequencies are filtered by $\phi_{2^J}(u) = 2^{-2J}\phi(2^{-J}u)$. For a Morlet Wavelet the averaging filter φ is chosen to be a Gaussian.

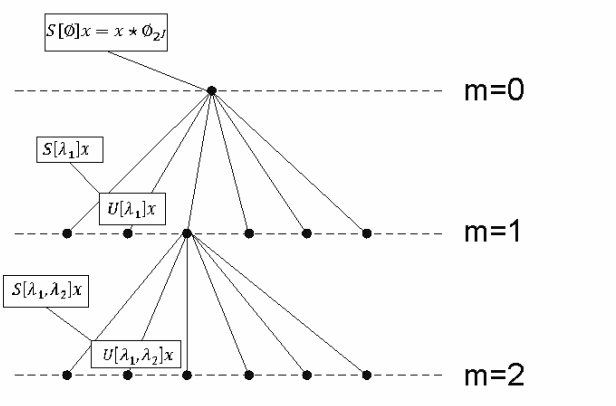

Fig. 2. A scattering propagator applied to x computes the first layer of wavelet coefficient modulus $U[\lambda]x$ and outputs its local average $S[\phi]x = x \star \phi_{2^J}$. Applying the propagator to the first layer coefficients $U[\lambda_1]$ outputs first-order scattering coefficients $S[\lambda_1]x$ and computes the propagated signal on the second layer $U[\lambda_1, \lambda_2]$

Figures 3 show an example of how the scattering transform can discriminate very different rainfalls: light rain and organized storm. The display of the scattering coefficients is as follows: orientation changes along the azimuth and the scale along the radius. The display of the second order coefficients follows the same rationale, see [4] for further details. Considering the power spectrum or the first order scattering coefficients does not allow an easy discrimination. On contrary, the second order scattering coefficients exhibit more energy for the organized storm.

4. FEATURES DESIGN

The scattering transform is performed with 6 scales and 12 orientations for a total of 2232 scattering coefficients (72 1^{st} order coefficients and 2160 2^{nd} order coefficients). 2^{nd} order scattering coefficients gather the most important information for the classification. The numbers of scales and orientations are those that give the best results on the considered database.

Figures 3 show that the orientation has a high influence in the scattering coefficients, especially the second order ones. This might indicate that the rain band has a particular shape which makes the scattering representation more powerful in

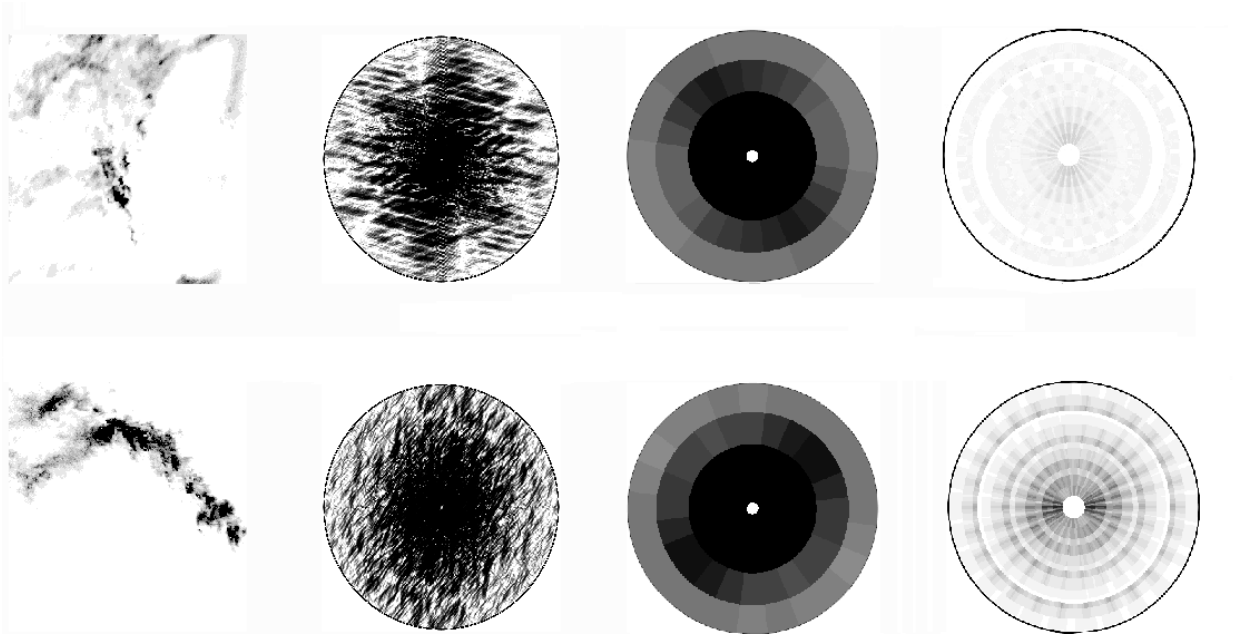

Fig. 3. Top figure: light rain. Bottom figure: organized storm. From left to right: radar image, power spectrum, first order scattering coefficients, and second order scattering coefficients.

a particular orientation. It is due to the wind direction which will be orthogonal to the most powerful signal direction. For example, typical fronts are moving from the South-West to the North-East in western Europe. This information can be meaningful to discriminate this class. However, we believe that the features shall be invariant to changes of orientation. Thus, the scattering coefficients are integrated over orientation as in [9]. So, there will be no more orientation components, but a unique coefficient defining the power for every scale. Also, thanks to this integration, the total number of coefficients is highly reduced: from 2232 to 21 scattering coefficients (6 1^{st} order coefficients and 15 2^{nd} order coefficients).

5. EXPERIMENTS

In order to evaluate the merit of the different representations discussed, a leave-one-out classification scheme is taken using the k-nearest neighbors algorithm [10] over a database of 1239 images, manually labeled in terms of rain type by visual inspection. The cardinality of the rain type classes is as follows: 497 images of light rain, 399 images of showers, 294 images of unorganized storms, and 49 images of organized storms.

Performance is measured using two metrics: the overall accuracy and the class wise accuracy. Overall accuracy is defined as the average number of correct predictions over the whole database with respect to the ground truth annotation. Class wise accuracy is the accuracy computed for each class and averaged over the classes. The latter is therefore independent of the distribution of the type of rainfall in the database.

	Accuracy	**Class acc.**
RID	89,43	85,17
Power Spectrum	72,72	58,51
1^{st} **order scattering**	90,88	88,93
2^{nd} **order scattering**	93,22	90,85
$1^{st} + 2^{nd}$ **order scattering**	93,46	91,47

Table 2. Overall performance.

The results achieved by the different methods can be seen on Table 2. Remember that the 1^{st} order scattering are conceptually equivalent to the SIFT, and can therefore be considered as a good baseline for texture classification. The RID features achieve good results with a drop in class wise accuracy. A closer look at the performance can be achieved by considering Table 3. For the largest class (Light rain), the performance is quite good, whereas organised storms are not well modeled, which affects the class wise accuracy. As storms exhibit spatial structure, one can expect that a frequency decomposition of the image might lead to better performance. This is not the case of the power spectrum, probably due to a lack of stability. The first order scattering performs better, while the second is considerably better. Considering the difference between the confusion matrices of the 1^st and 2^nd orders shown on respectively Tables 4 and 5, we see that the classes which require a finer modeling of the spatial structure are better handled by the latter. This is probably due to the fact that higher order statistics are nicely encoded by the 2^nd

	Rain	Shower	U. Storm	O. Storm
Rain	**98,2**	0,2	1,6	0,0
Shower	0,0	**89,7**	10,0	0,3
U. Storm	1,7	17,4	**78,9**	2,0
O. Storm	0,0	6,1	26,5	**67,4**

Table 3. Confusion matrix of the RID statistics.

	Rain	Shower	U. Storm	O. Storm
Rain	**97,6**	1,2	1,2	0,0
Shower	3,3	**87,7**	7,5	1,5
U. Storm	1,7	13,6	**84,7**	0
O. Storm	0,0	8,2	6,1	**85,7**

Table 4. Confusion matrix of the 1^{st} order scattering coefficients.

order scattering coefficients.

Further, applying a Principal Components Analysis (PCA) over the scattering transform integrated over rotation, (both 1^st and 2^nd scattering coefficients) leads to 11 principal components which further improve performance. The combination of those features with the RID statistics further achieve a satisfactory score of almost 98 % in accuracy and class wise accuracy, which tends to demonstrate the complementarity of distribution based features, and spatial based features.

6. CONCLUSION

Satisfactory results reported in this paper show the relevance of the use of the scattering transform to predict the rainfall type from rainfall intensity radar measurements. of the scattering transform for classifying the radar images used in rainfall prediction. It is expected to be relevant when classifying new radar images. It has also been demonstrated that the RID statistics of the images and the scattering transform have complementary information which, if jointly considered, achieve a high classification score when merging both information on the studied database. Future work will consist in considering more principled classification schemes such as the Support Vector Machines (SVM)s over a larger scale database and comparing with other state of the art local features commonly used for texture classification [11].

	Rain	Shower	U. Storm	O. Storm
Light rain	**99,0**	0,6	0,4	0,0
Shower	1,2	**91,7**	6,3	0,8
U. Storm	1,4	11,2	**87,4**	0,3
O. Storm	0,0	2,0	10,2	**87,8**

Table 5. Confusion matrix of the 2^{nd} order scattering coefficients.

	Accuracy	Class accuracy
PCA Scattering	93,87	92,24
RID + Scattering	97,18	96,22
RID + PCA Scat	98,22	97,95

Table 6. Performance of enhanced feature sets.

REFERENCES

[1] S. Lovejoy and B. B. Mandelbrot, "Fractal properties of rain, and a fractal model," *Tellus A*, vol. 37A, no. 3, pp. 209–232, 1985.

[2] S. Lovejoy and D. Schertzer, "Generalized scale invariance in the atmosphere and fractal models of rain," *Water Resources Research*, vol. 21, no. 8, pp. 1233–1250, 1985.

[3] I. Emmanuel, H. Andrieu, E. Leblois, and B. Flahaut, "Temporal and spatial variability of rainfall at the urban hydrological scale," *Journal of Hydrology*, vol. 430431, no. 0, pp. 162 – 172, 2012.

[4] S. Mallat, "Group invariant scattering," *Communications on Pure and Applied Mathematics*, vol. 65, no. 10, pp. 1331–1398, 2012.

[5] J. Bruna and S. Mallat, "Invariant scattering convolution networks," *IEEE Transactions on Pattern Analysis and Machine Intelligence*, vol. 35, no. 8, pp. 1872–1886, Aug 2013.

[6] Alexis Berne, Guy Delrieu, Jean-Dominique Creutin, and Charles Obled, "Temporal and spatial resolution of rainfall measurements required for urban hydrology," *Journal of Hydrology*, vol. 299, no. 34, pp. 166 – 179, 2004.

[7] I. Emmanuel, H. Andrieu, and P. Tabary, "Evaluation of the new french operational weather radar product for the field of urban hydrology," *Atmospheric Research*, vol. 103, no. 0, pp. 20 – 32, 2012.

[8] David G. Lowe, "Distinctive image features from scale-invariant keypoints," *International Journal of Computer Vision*, vol. 60, no. 2, pp. 91–110, 2004.

[9] L. Sifre and S. Mallat, "Rotation, scaling and deformation invariant scattering for texture discrimination," in *IEEE Conference on Computer Vision and Pattern Recognition*, 2013, pp. 1233–1240.

[10] T. Cover and P. Hart, "Nearest neighbor pattern classification," *IEEE Transactions on Information Theory*, vol. 13, no. 1, pp. 21–27, January 1967.

[11] K. Mikolajczyk and C. Schmid, "A performance evaluation of local descriptors," *IEEE Transactions on Pattern Analysis and Machine Intelligence*, vol. 27, no. 10, pp. 1615–1630, Oct 2005.